DOI: 10.30511/pcdp.2024.718345 - ISSN: 3060-8376 - Vol 1(1), 2024

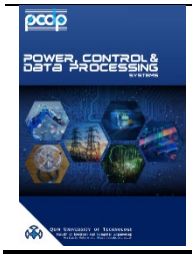

POWER, CONTROL AND DATA PROCESSING SYSTEMS

Available Online at: https://pcdp.qut.ac.ir/

Optimal Operation of Solar Energy System integrated with Energy Storage Systems

ARTICLE INFO

Article Type
Original Research

Authors
Mohammad Reza Masoudi[1]
Mehran Haghighi[1,*]
Milad Rahimipour Behbahani[2]

[1] Department of Power and Control Engineering, School of Electrical and Computer Engineering, Shiraz University, Shiraz, Iran,
mohammadreza.masoudi@hafez.shirazu.ac.ir,
mehranhaghighi@hafez.shirazu.ac.ir
[2] Department of Electrical Engineering and Information Technology, Ilmenau University of Technology, Germany,
milad.rahimipour-behbahani@tu-ilmenau.de

*** *Correspondence***
Address: Department of Power and Control Engineering, School of Electrical and Computer Engineering, Shiraz University, Shiraz, Iran
Phone: -
Fax: -
mehranhaghighi@hafez.shirazu.ac.ir

Article History
Received: October 30, 2024
Accepted: November 22, 2024
ePublished: December 01, 2024

ABSTRACT

One of the most pressing challenges in power systems is the environmental impact, which is so critical that the Smart Grid (SG) includes it as one of the three key pillars in its framework. Renewable energy sources offer a potential solution by reducing reliance on fossil fuels and lowering carbon dioxide emissions, which are detrimental to the environment and contribute to global warming. However, certain renewable sources, such as photovoltaic (PV) cells, have uncontrollable power generation, posing a new challenge for grid stability. A viable solution to this issue is the implementation of Energy Storage Systems (ESS). These systems can store excess energy produced by renewables during periods of overproduction and release it when needed to enhance economic operation. In this paper, a Unit Commitment (UC) problem is performed in the presence of PV cells, ESS (in the form of batteries), and imported power from neighboring grids. The problem is modeled and simulated in MATLAB, where the inherent nonlinearity is managed by applying a Mixed-Integer Linear Programming (MILP) approach. Also, the simulation framework is designed with flexibility, enabling it to accommodate various piecewise linearization and different configurations of thermal units in the grid. The simulation results demonstrate an optimal economic operation with a total cost of approximately 124.57 $/MWh achieved through effective integration of solar energy and energy storage systems.

Keywords: Energy Storage System (ESS); Mixed integer linear programming (MILP); photovoltaic (PV); Unit commitment (UC); Optimal operation; Smart grid (SG).

1 Introduction

The first electric power network was established between 1885 and 1895, and for a long time, the electrical energy system underwent minimal change. However, recent advancements signal the onset of a new era. Over time, the number of power grids has increased to the point where there are now more than 9,200 grids worldwide, supplying approximately one million megawatts of power to consumers. As with other technologies, the evolution of power grids is inherently linked to temporal progress; thus, digital technologies are now being integrated into power systems to enhance network efficiency. This digital integration facilitates two-way communication, ensuring a direct connection between generation and consumption. Therefore, when information technology is added to the existing network constitutes what is termed a Smart Grid (SG) [1]. The concept implies that for a grid to be smart, it must be capable of two-way power and information transfer, network control and monitoring, and ensuring continuous and reliable power supply to consumers [2].

When comparing traditional grid operations with smart grids, it is observed that in traditional operations, two main factors, economic efficiency and reliability, have been prioritized. However, in smart grids, in addition to these factors, environmental sustainability is also incorporated as a priority. Fossil fuels have been predominantly used for power generation, causing global warming and environmental pollution. Therefore, renewable energy (RE) sources are increasingly integrated into smart grids [3].

Smart grids represent an evolution of traditional power systems, integrating advanced technologies to enhance efficiency, reliability, and sustainability [4]. Unlike conventional grids that primarily focus on economic efficiency and reliability, smart grids also emphasize environmental sustainability by facilitating the integration of RE sources [5]. This integration helps reduce greenhouse gas emissions and addresses the exhaustion of fossil fuels [6]. However, the intermittent nature of renewable sources poses challenges to grid stability and management [5]. Smart grids incorporate innovative technologies such as two-way communication, automated controls, and forecasting systems to overcome these challenges and optimize energy usage [4]. Additionally, smart grids enable decentralized and localized power generation, reducing transmission costs and improving reliability [6]. Despite these advantages, the integration of renewables into smart grids requires addressing various technical, operational, and market-related issues to ensure successful implementation [7].

Smart grids, despite their advantages, are faced with challenges such as adequacy under uncertainty, net load ramp management, network congestion, and voltage and frequency stability. Solutions like demand response and ESS are proposed to tackle these issues. The importance of ESS has become so significant today that numerous studies are now focused on estimating the charging and discharging profiles of electric vehicles connected to the grid [8]. Additionally, smart homes and smart grids are supported through load commitment (LC) [9].

The UC problem is addressed by determining which units should operate or shut down at specific times [10, 11]. The optimal power output for each unit, considering RE, ESS, and imported power, is decided [12]. UC problems have been identified as practically significant due to their economic impact on power companies. Various methods have been explored for solving UC problems, with heuristic algorithms showing promising results. However, challenges, such as parameter tuning, are recognized when heuristic approaches are applied [10].

Several algorithms have been explored for solving the UC problem, each with distinct advantages and disadvantages. Heuristic methods like genetic algorithms (GA) and particle swarm optimization (PSO) are popular for their flexibility and ease of implementation [13,14]. However, their main drawback is that they often converge to local optima instead of finding the global optimum, especially when the problem size increases or when complex constraints, such as minimum on/off times and ramp rates, are involved. Additionally, these methods require extensive parameter tuning, which can be time-consuming and may not always yield the best results.

Metaheuristic algorithms, such as Tabu Search and Simulated Annealing, offer better convergence properties than simple heuristics, but they also come with drawbacks [15, 16]. While these methods are less likely to get stuck in local optima, they can be computationally expensive, particularly for large-scale UC problems. The quality of the solution often depends on the initialization settings and control parameters, and these algorithms might require a longer time to find a near-optimal solution, which can be impractical for real-time decision-making in dynamic power systems.

Dynamic programming (DP), a classical optimization method, is known for its ability to guarantee the optimal solution [17]. However, it suffers from the "curse of dimensionality," meaning its computational cost grows exponentially as the problem size increases. This makes DP impractical for large UC problems, especially when dealing with grids that include many generating units and renewable energy sources. Moreover, it requires significant memory and computational resources, which limits its applicability in real-world scenarios.

MILP has emerged as a more balanced and efficient approach for UC problems. One of the key advantages of MILP is its ability to handle large-scale systems with complex, non-linear constraints while still finding the global optimum. With recent advancements in MILP solvers, the computational time has been significantly reduced, making it suitable for real-time and large-scale applications. Therefore, MILP provides more accurate and stable solutions compared to heuristic and metaheuristic methods. These advancements in MILP solvers have significantly improved the efficiency and accuracy of solving UC problems. These solvers allow for precise modelling of complex system dynamics, such as start-up costs,

ramp rates, and minimum on/off times, which are critical in optimizing thermal unit operations [10]. The integration of renewable energy sources, like wind and solar, has increased uncertainty in power generation, and MILP solvers have proven effective in managing these challenges by optimizing power generation schedules despite the variability in renewable outputs [11]. Furthermore, MILP has been instrumental in enhancing the coordination between ESS and generation units, ensuring grid reliability while minimizing operational costs [18]. The ability of MILP to handle large-scale systems with complex constraints has made it a popular choice for UC problems, offering practical solutions that directly impact modern power systems [19].

In this paper, the authors contribute to UC problem under the presence of RE sources, specifically PV systems, and ESS in the form of batteries. The study employs a MILP approach to handle the inherent nonlinearity of the UC problem. Furthermore, imported power from neighbouring grids is incorporated into the model. A significant aspect of this work is the piecewise linearization of thermal unit cost functions, approximating them into 1000 linear segments to achieve computational efficiency without sacrificing accuracy. The flexible MATLAB simulation framework allows for the adjustment of parameters such as the number of segments and generators, enabling adaptability for various grid configurations. The findings highlight the economic benefits of utilizing renewable energy during available hours and the critical role of ESS in enhancing grid stability by storing excess energy and releasing it when needed, thereby supporting the goals of the Smart Grid in reducing reliance on fossil fuels and promoting environmental sustainability.

The contributions of this paper can be summarized as follows:

- Addressing UC Problem with Renewables: Incorporates renewable energy sources, specifically photovoltaic (PV) systems, into the UC problem framework.
- Integration of ESS: Models the role of batteries for storing excess energy and releasing it during demand peaks, enhancing grid stability.
- Inclusion of Imported Power: Integrates imported power from neighboring grids to ensure reliable and flexible operation.
- MILP Approach for Nonlinearity: Employs a MILP approach to handle the inherent nonlinearity of the UC problem.
- Piecewise Linearization of Cost Functions: Implements piecewise linearization of thermal unit cost functions into 1000 segments to improve computational efficiency while maintaining accuracy.
- Flexible Simulation Framework: Develops a MATLAB-based framework capable of adjusting parameters such as the number of segments and generators, enabling adaptability for various grid configurations.

Economic and Environmental Impact: Demonstrates the economic benefits of renewables and highlights the role of ESS in reducing reliance on fossil fuels, aligning with Smart Grid sustainability goals.

The rest of the paper is organized as follows:

- Mathematical modeling of the system
- Problem formulation
- Simulations and results
- Conclusion

2 Mathematical modeling of the system

Photovoltaic (PV) cells and batteries, functioning as energy storage units, play a crucial role as integrated subsystems within the broader framework of a Smart Grid. These components serve distinct yet complementary purposes: PV cells harness renewable solar energy, converting sunlight into electricity, while batteries store excess energy for later use, helping to balance supply and demand. The integration of these subsystems into the power grid enhances grid stability and efficiency, as they can mitigate the variability inherent in renewable energy generation. This section delves into the detailed mathematical modeling of these two subsystems, addressing their operational characteristics, interactions with other grid elements, and the constraints that govern their performance within the overall power system.

2.1 Modeling of Photovoltaic (PV) Cells

A PV cell operates as a renewable energy source by converting sunlight into electrical power. The efficiency of a PV cell, denoted by η_{pv}, determines the proportion of solar energy converted into electricity, while the area A_{pv} represents the physical surface exposed to sunlight. Solar irradiance, represented by R_t, refers to the intensity of sunlight at a given time. The power output of a PV cell is directly proportional to these factors, meaning that higher irradiance or a larger surface area will increase the energy production, assuming constant efficiency. The power output at any given hour t is modeled by the following equation:

$$p_{pv_t} = R_t . A_{pv} . \eta_{pv} \qquad \text{Eq 1}$$

This equation quantifies the power generated by the PV cell, taking into account the irradiance at any particular moment, the area of the solar array, and the conversion efficiency of the system. By adjusting the parameters, this model can predict the energy output under different weather conditions and system configurations.

2.2 Modeling of the Energy Storage System (ESS)

The energy storage system consists of a battery. Since a battery cannot simultaneously charge and discharge, two binary variables, B_t^{ch} for charging and B_t^{dch} for discharging, are introduced to ensure this condition. The battery introduces constraints to the optimization problem. The terms SOC (State of Charge) and DOD (Depth of Discharge) describe the battery's state. SOC represents the current charge level relative

to the battery's total capacity, while DOD indicates the extent of discharge relative to its nominal capacity. It is important to note that not all of a battery's nominal capacity is usable; fully discharging the battery can lead to irreversible damage. Therefore, a portion of the nominal capacity is considered inactive. Let η_s represent battery efficiency, Δt the simulation time step (one hour), and C_s the battery capacity. The state of charge can be expressed by the following equation:

$$SOC_t = \frac{\eta_s \Delta t}{C_s} p_t^{ch} - \frac{\Delta t}{C_s \eta_s} p_t^{dch} + SOC_{t-1} \quad \text{Eq 2}$$

$$(1 - DOD_{max}) \leq SOC_t \leq SOC_{max} \quad \text{Eq 3}$$

Equation (3) provides an important inequality constraint for the battery. By combining Equations (2) and (3), the following relations (4) and (5) can be derived:

$$\frac{\eta_s \Delta t}{C_s} p_t^{ch} - \frac{\Delta t}{C_s \eta_s} p_t^{dch} \leq SOC_{max} - SOC_{t-1} \quad \text{Eq 4}$$

$$\frac{\Delta t}{C_s \eta_s} p_t^{dch} - \frac{\eta_s \Delta t}{C_s} p_t^{ch} \leq DOD_{max} - 1 + SOC_{t-1} \quad \text{Eq5}$$

$$B_t^{ch} + B_t^{dch} \leq 1 \quad \text{Eq 6}$$

$$p_t^{ch} - p_{max}^{ch} B_t^{ch} \leq 0 \quad \text{Eq 7}$$

$$p_t^{dch} - p_{max}^{dch} B_t^{dch} \leq 0 \quad \text{Eq 8}$$

Equations (6), (7), and (8) ensure that charging and discharging do not occur simultaneously. Additionally, constraints related to p_{max}^{ch} and p_{max}^{dch}, which represent the maximum charging and discharging power within each Δt, are included. Equation (7) applies when the charging binary is active, and Equation (8) applies when the discharging binary is active.

3 Problem formulation

3.1 Objective Function

The objective function of this study is the minimization of total daily operational cost, represented as f^T:

$$f^T = \sum_{t=1}^{J} \{ \sum_{i=1}^{N_{TG}} (\sum_{k=1}^{N} S_{ik} p_{TG_{ikt}} + F_{C_i}(p_{TG_i}^{min}) U_{it} + SUC_{TG_i} Y_{it}) \} \quad \text{Eq 9}$$

In the above equation, J indicates the total number of scheduling hours, N_{TG} denotes the number of available thermal generators in the network. The nonlinear characteristics of these generators are observed in Equation (10), where a piecewise linear approximation must be applied for solving using the MILP method. Here, N represents the number of segments used in the conversion from nonlinear to linear. The slope of each linear segment is denoted as S and P_{TG} indicates the thermal generators' power for each linear segment. The cost function of generator i is expressed as F_{C_i}, $p_{TG_i}^{min}$ is the minimum power of the i-th generator, U_{it} is the binary variable indicating the on/off status of the i-th unit, SUC_{TG_i} is the startup cost of the i-th unit and Y_{it} is the binary variable for the startup cost.

$$F_{C_i}(p_{TG_{it}}) = c_i + b_i p_{TG_{it}} + a_i {p_{TG_{it}}}^2 \quad \text{Eq 10}$$

3.2 Constraints of the UC Problem

A. Power Balance

The sum of the output power from the generating units, the power output from the PV system, the charging and discharging power of the ESS, and the imported power must exactly meet the load demand for each hour. Thus, Equation (11) expresses the power balance constraint for hour t:

$$\sum_{i=1}^{N_{TG}} \sum_{k=1}^{N} p_{TG_{ikt}} + \sum_{i=1}^{N_{TG}} p_{TG_i}^{min} U_{it} + p_{pv_t} + p_{IMP_t} - p_t^{ch} + p_t^{dch} = p_{ld_t} \quad \text{Eq 11}$$

In this equation, p_{pv_t} represents the power generated from solar cells in hour t, p_{IMP_t} indicates the imported power from neighboring countries in hour t, p_t^{ch} is the charged power of the battery in hour t, p_t^{dch} is the discharged power of the battery in hour t and p_{ld_t} denotes the consumed load in hour t.

B. Binary Generator

To solve the UC problem, a constraint relating to the binary variables is required, this constraint is represented in Equation (12):

$$Z_{it} = Y_{it} + U_{i(t-1)} - U_{it} \quad \text{Eq 12}$$

C. Power Generation

Given that the problem has transitioned from a nonlinear to a linear state, the sum of the production capacities, which serve as the decision variables, must remain within their minimum and maximum limits for each thermal unit. Ensuring the binary state of the thermal units is crucial in this constraint to maintain a linear objective function and avoid nonlinearity caused by variable multiplication. This constraint can be expressed as follows:

$$p_{TG_i}^{min} U_{it} \leq \sum_{k=1}^{N} p_{TG_{ikt}} \leq p_{TG_i}^{max} U_{it} \quad \text{Eq 13}$$

D. Up and Down:

Additional constraints significant to this problem are the up and down constraints. These apply when a thermal unit needs to turn on or off. Specifically, when a unit is turned on, it must remain operational for a specified up time, and when turned off, it must stay inactive for a specified down time. The mathematical representations of these constraints are provided in Equations (15), (16), and (17). Equation (14) indicates that the binary variables for on and off states cannot be simultaneously active:

$$Y_{it} + Z_{it} \leq 1 \quad \text{Eq 14}$$

$$\sum_{k=t-up_i+1}^{t} Y_{ik} \leq U_{it} \quad \text{Eq 15}$$

$$\sum_{k=t-dn_i+1}^{t} Z_{ik} \leq 1 - U_{it} \quad \text{Eq 16}$$

$$U_{it} - U_{i(t-1)} \leq Y_{it} \quad \text{Eq 17}$$

Battery constraints are outlined in the mathematical modeling section, observable in Equations (2) through (8).

3.3 Optimization Method

A MILP solver is employed for this optimization problem, utilizing various techniques to identify the optimal solution of the objective function $f^T x$, where f is a vector of linear coefficients, and x is the solution vector. The linear constraints form the conditions for the MILP, excluding any nonlinear

limitations. Specifically, constraints exist for the integer variables in x. For the given objective function f, the inequality matrices A_{ineq} and equality matrices A_{eq}, alongside the inequality vector b_{ineq} and equality vector b_{eq} and upper and lower bounds u_b, l_b define the problem model for deriving the solution vector xxx from the feasible solution space, as represented in Equation (18):

$$\min f^T x \; subject\; to \begin{cases} x(intcon) are\; integers \\ A_{ineq}.x \le b_{ineq} \\ A_{eq}.x = b_{eq} \\ l_b \le x \le u_b \end{cases} \quad \text{Eq 18}$$

The MILP algorithm utilizes six strategies to solve optimization problems effectively. If a solution is found in one step, the algorithm does not continue to the next step. The main strategies are outlined as follows:

- Reducing the problem size through linear programming preprocessing.
- Solving an initial relaxed (non-integer) problem using linear programming.
- Performing preprocessing of the mixed-integer programming problem to tighten the LP relaxation.
- Attempting to use cutting-plane methods to tighten the LP relaxation of the mixed-integer programming problem.
- Employing heuristic methods to find feasible integer solutions.
- Utilizing a branch-and-bound algorithm for systematic search of the optimal solution.

4 Simulation and results

In this section, the proposed power system is described in detail. The case study focuses on the IEEE 30-bus system [20]. Figure 1 provides an illustration of this standard network. The UC problem will be simulated for 6 thermal units (as shown in Figure 2), 1 solar unit serving RE, 1 battery acting as the ESS, and imported power. The general layout of the tested system can also be observed in Figure 2.

The thermal units in the 30-bus system feature nonlinear cost functions. A more detailed overview of these thermal units can be found in Figures 3, 4, and 5. Figure 3 depicts the minimum and maximum power outputs of the units, Figure 4 outlines the startup costs for each thermal unit, and Figure 5 presents the minimum up and down times (i.e., the minimum time a unit must stay online after being turned on, and offline after being turned off).

The total power generated by PV over 24 hours, using Equation (1) and the solar irradiance from Figure 6, is shown in Figure 7. The efficiency is set at 40%, and the PV cell area is considered to be 400,000 m². The battery parameters for this study are summarized in Table 1. As is well known, one of the most important elements of a network is the load. In this specific study, the load behavior is observed, and Figure 8 has been prepared to illustrate this behavior. The imported power for this particular study has been considered constant at 100 MW per hour.

Table 1. ESS Parameters

Parameter	Value
η_s	0.9
$C_s(MW)$	25
SOC_{max}	0.95
DOD_{max}	0.95
$p_{max}^{ch}(MW)$	20
$p_{max}^{dch}(MW)$	10

The simulations were carried out on a system equipped with an Intel Core i7 CPU and 16 GB of RAM, utilizing MATLAB R2023a. The computational environment allowed for efficient processing of the required models and data. MATLAB's advanced toolboxes and functionalities were leveraged to ensure accurate simulation results, which were essential for the analysis and validation of the proposed methods in this study. Figure 9 illustrates an overall flowchart of the proposed optimization.

Table 2 summarizes the overall results of the simulation over a 24-hour period. In this table p_{GT1}, p_{GT2}, p_{GT3}, p_{GT4}, p_{GT5}, p_{GT6} represent the power generated by thermal units 1 through 6 at hour t. Additionally, $U_1U_2U_3U_4U_5U_6$ are the binary variables indicating whether each thermal unit is on during hour t, and $Y_1Y_2Y_3Y_4Y_5Y_6$ are the startup binaries for these units at the same hour. $Z_1Z_2Z_3Z_4Z_5Z_6$ indicate the shutdown binaries for the units.

The binary variables $B_{sh}B_{dsh}$ correspond to the battery's charging and discharging statuses at hour *t*. As mentioned earlier, both variables are necessary to avoid simultaneous charging and discharging of the battery. The variables p_{sh} and p_{dsh} represent the charging and discharging power when the respective binary is active. A quick glance at Table 2 reveals that the third unit did not operate during any hour. This can be explained by Figure 4, which illustrates the startup costs of the units. The startup cost of the third unit is the highest among all, making it economically inefficient. Table 2 also confirms compliance with all the constraints mentioned, the most significant being the power balance constraint, as described in Equation (11). This constraint can be analyzed based on Table 2, Figures 3, 7, and 8, ensuring its validity. Furthermore, the binary variables for the thermal units are shown to be activated correctly according to Table 2. As highlighted in this table, during the hours when solar power—referenced in Figure 7—along with imported power, is sufficient to meet the load, as shown in Figure 8, any excess power can be stored in the battery due to the uncontrollable nature of solar energy. The stored energy can then be utilized in subsequent hours when needed, allowing for the contribution of more economically viable units. Figure 10 presents the SOC of the battery at different hours, with the peak occurring at hour 12. Finally, the battery's SOC returns to its initial level. Figure 10 illustrates the SOC, charge and discharge power of the battery over a 24-hour period. In this chart, it is evident that the battery remains mostly uncharged during the early hours of the day (hours 1 to 10). At hour 11, the battery charge rapidly increases, reaching its peak, and then gradually discharges. This behavior indicates that the battery is charged to support the grid demand

during peak hours and subsequently discharged during off-peak hours to assist the generating units. This energy management strategy helps reduce operational costs and enhances grid stability.

5 Conclusion

In this paper, a UC problem was simulated in the presence of PV cells as a renewable energy source, alongside battery storage and imported power from neighbouring grids. The findings highlight the significant potential of utilizing renewable energy, particularly during hours when solar power can be harnessed economically. The simulation demonstrates that the integration of renewable energy, combined with imported power, can help maintain power balance, especially in networks facing production shortages. Additionally, the implementation of ESS, specifically batteries, is crucial for enhancing the intelligence of our grid. These systems enable the storage of uncontrollable renewable energy during periods of excess generation and facilitate its release during times of need. The use of MILP to address the inherent nonlinearity of the problem allows for an efficient and flexible solution framework. This approach provides the advantage of accommodating various configurations of thermal units and piecewise linearization, making the model adaptable to different scenarios. Overall, the incorporation of renewable energy sources, energy storage solutions, and imported power aligns with the objectives of smart grid development. It fosters a sustainable energy future by providing economic benefits while also addressing the pressing issue of environmental impact, ultimately contributing to a more resilient and intelligent energy network.

Future work directions based on this study include the following:

- Dynamic Pricing Analysis: Investigating the impact of dynamic electricity pricing on the optimal scheduling of renewable energy, ESS, and imported power.
- Advanced ESS Technologies: Exploring the integration of emerging energy storage technologies, such as flow batteries or hydrogen storage, to improve system performance.
- Real-Time Implementation: Developing real-time optimization frameworks to enhance the adaptability of the model to rapid changes in grid conditions.
- Multi-Objective Optimization: Extending the model to include multi-objective optimization criteria, such as minimizing emissions and maximizing reliability alongside cost reduction.
- Grid Expansion Studies: Examining the impact of integrating additional renewable energy sources, such as wind power, and expanding the grid's capacity for future energy demands.
- Decentralized Energy Management: Investigating decentralized or distributed energy management approaches for microgrids using similar modeling frameworks.

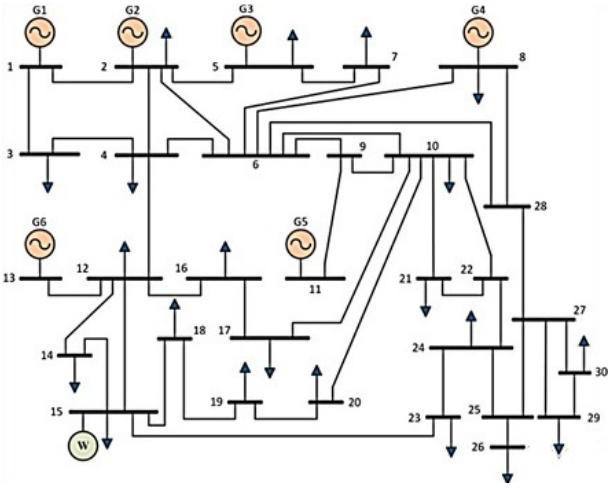

Fig. 1. The IEEE 30-bus system [20].

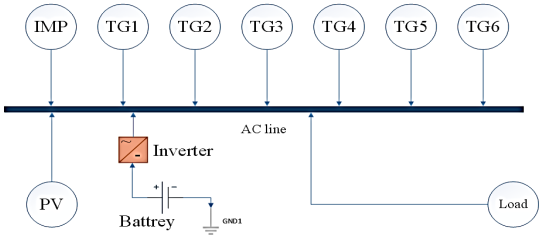

Fig. 2. The general layout of the purposed system.

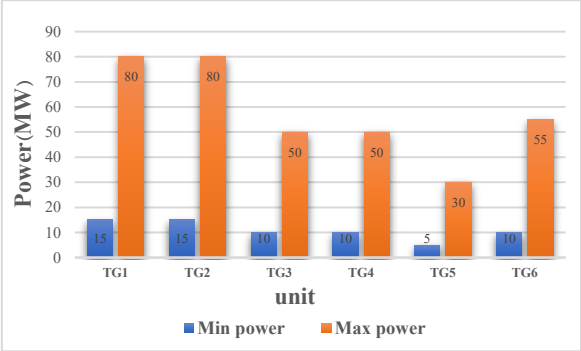

Fig. 3. Minimum and maximum power outputs of thermal units.

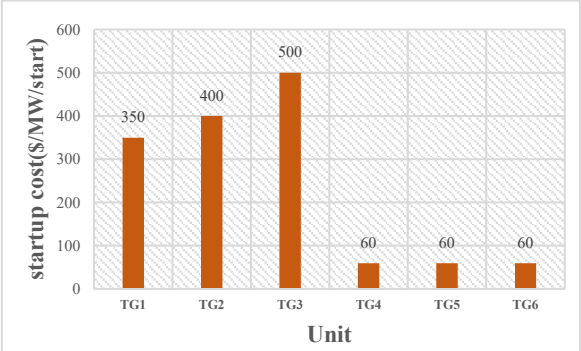

Fig. 4. Startup costs for each thermal unit.

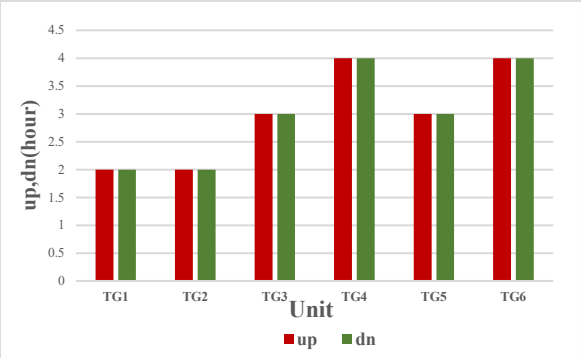

Fig. 5. The minimum up and down times.

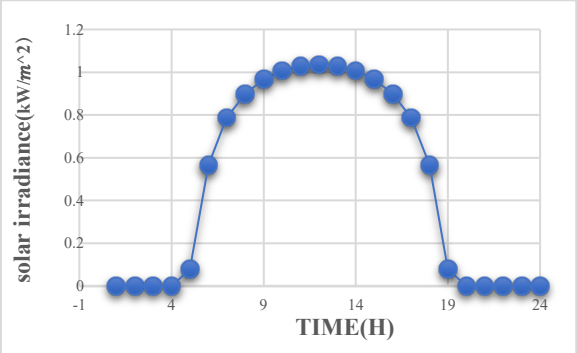

Fig. 6. Solar irradiance.

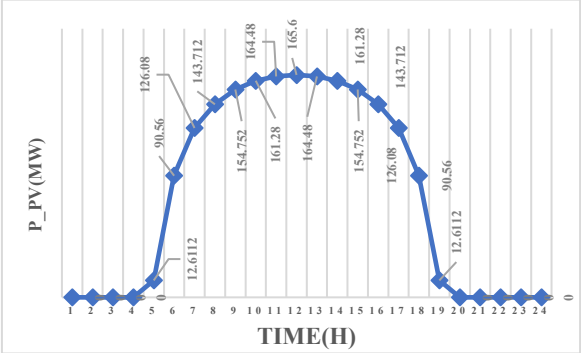

Fig. 7. Power generated by PV.

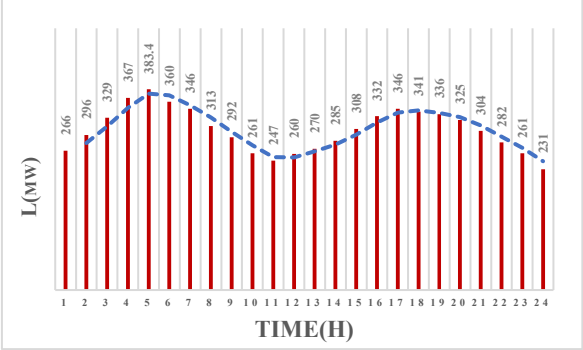

Fig. 8. Load

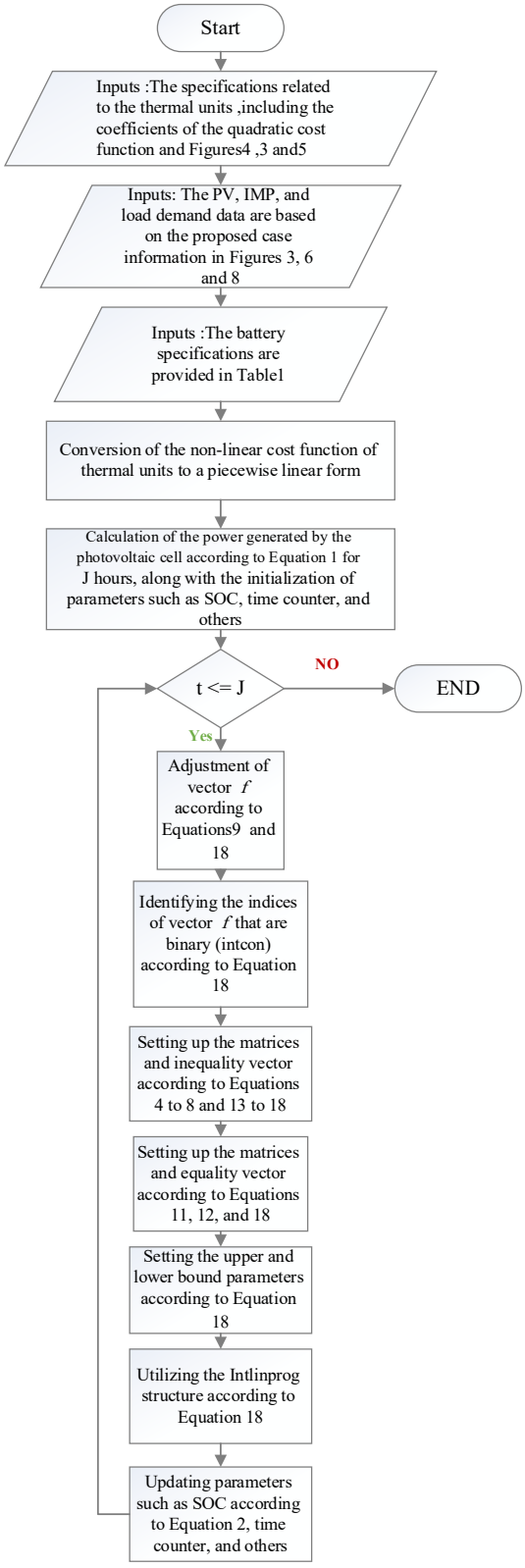

Fig. 9. overall flowchart

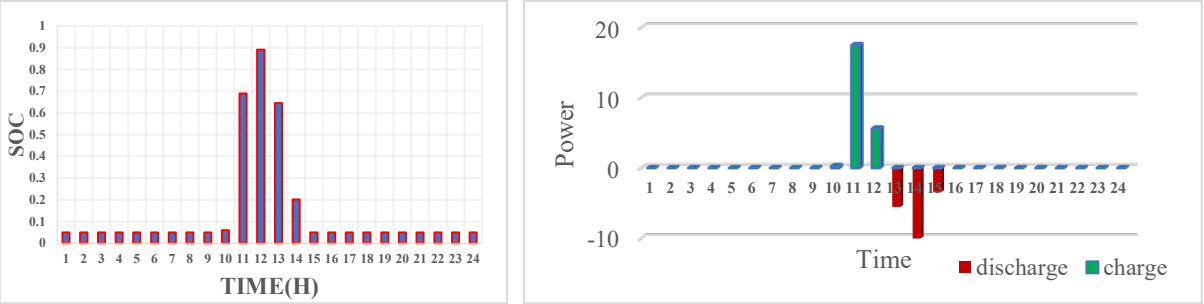

Fig. 10. SOC, charge and discharge power of battery.

Table 2. Result of simulation

t	p_{GT1}	p_{GT2}	p_{GT3}	p_{GT4}	p_{GT5}	p_{GT6}	$U_1U_2U_3U_4U_5U_6$	$Y_1Y_2Y_3Y_4Y_5Y_6$	$Z_1Z_2Z_3Z_4Z_5Z_6$	$B_{sh}B_{dsh}$	p_{sh}	p_{dsh}
1	77	0	0	34	0	55	100101	100101	000000	00	0	0
2	77	0	0	34	30	55	100111	000010	000000	00	0	0
3	54	69	0	26	25	55	110111	010000	000000	00	0	0
4	72	80	0	30	30	55	110111	000000	000000	00	0	0
5	73.5	80	0	32.29	30	55	110111	000000	000000	00	0	0
6	34.94	47.5	0	22	10	55	110111	000000	000000	00	0	0
7	30	32.92	0	20	0	37	110101	000000	000010	00	0	0
8	0	32.29	0	0	0	37	010001	000000	100100	00	0	0
9	0	37.25	0	0	0	0	010000	000000	000001	00	0	0
10	0	0	0	0	0	0	000000	000000	010000	10	0.28	0
11	0	0	0	0	0	0	000000	000000	000000	10	17.48	0
12	0	0	0	0	0	0	000000	000000	000000	10	5.6	0
13	0	0	0	0	0	0	000000	000000	000000	01	0	5.52
14	0	0	0	0	13.72	0	000010	000010	000000	01	0	10
15	0	0	0	0	10	39.85	000011	000001	000000	01	0	3.4016
16	0	0	0	22	11.29	55	000111	000100	000000	00	0	0
17	0	0	0	34.92	30	55	000111	000000	000000	00	0	0
18	49.44	0	0	26	20	55	100111	100000	000000	00	0	0
19	54	67	0	26	21.39	55	110111	010000	000000	00	0	0
20	54	67	0	26	23	55	110111	000000	000000	00	0	0
21	47.5	60.5	0	22	19	55	110111	000000	000000	00	0	0
22	41	54	0	22	10	55	110111	000000	000000	00	0	0
23	34.5	41.5	0	20	10	55	110111	000000	000000	00	0	0
24	30	34.5	0	20	0	46.5	110101	000000	000010	00	0	0

Parameters and Symbols

x: Solution vector $f^T x$: Total cost function A_{ineq}: Coefficients of variables in the inequality constraint in standard form b_{ineq}: Constant terms in the inequality constraint in standard form A_{eq}: Coefficients of variables in the equality constraint in standard form b_{eq}: Constant terms in the equality constraint in standard form l_b: Lower bounds of variables u_b: Upper bounds of variables J: Total simulation time N_{TG}: Total number of thermal power plants	N: Number of piecewise linearizations of the cost function for a thermal plant p_{pv_t}: Power generated by the photovoltaic cell at time t p_{IMP_t}: Power imported from neighboring grids at time t p_t^{ch}: Charging power of the ESS at time t p_t^{dch}: Discharging power of the ESS at time t p_{ld_t}: Load demand at time t $p_{TG_i}^{min}$: Minimum power the i-th thermal plant can generate $p_{TG_i}^{max}$: Maximum power the i-th thermal plant can generate SUC_{TG_i}: Startup cost of the i-th thermal unitS_{ik}: Slope of the linearized cost function for the i-th thermal plant and the k-th linearized segment F_{C_i}: Cost function of the i-th thermal plant $p_{TG_{ikt}}$: Power generated by the k-th segment of the i-th thermal plant at time t

Abbreviations

MILP : Mixed-Integer Linear Programming	PV : Photovoltaic	SG : Smart Grid	RE : Renewable Energy
UC : Unit Commitment	ESS : Energy Storage System	LC : Load Curtailment	

Disclosure of Potential Conflicts of Interest

The Authors declare that there is no conflict of interest

Reference

[1] V. Kulkarni, S. K. Sahoo, S. B. Thanikanti, S. Velpula, and D. I. Rathod, "Power systems automation, communication, and information technologies for smart grid: A technical aspects review," *TELKOMNIKA (Telecommunication Computing Electronics and Control)*, vol. 19, no. 3, p. 1017, Apr. 2021.

[2] S. Kumar, U. Yadav, M. Kumar, and J. D. Kumar, Understanding SMART GRID Power System: A review of network Architecture. 2024.

[3] M. H. Rehmani, M. Reisslein, A. Rachedi, M. Erol-Kantarci, and M. Radenkovic, "Integrating renewable energy resources into the smart grid: recent developments in information and communication technologies," IEEE Transactions on Industrial Informatics, vol. 14, no. 7, pp. 2814–2825, Mar. 2018.

[4] M. A. Mohamed, A. M. Eltamaly, H. M. Farh, and A. I. Alolah, Energy management and renewable energy integration in smart grid system. 2015.

[5] Zafar, Salman and Khalid Nawaz. "INTEGRATION OF RENEWABLE ENERGY SOURCES IN SMART GRID: A REVIEW." (2013).

[6] H. J. Bhatti and M. Danilovic, "Making the world more sustainable: Enabling localized energy generation and distribution on decentralized smart grid systems," World Journal of Engineering and Technology, vol. 06, no. 02, pp. 350–382, Jan. 2018.

[7] Z. Ullah et al., "Renewable Energy Resources Penetration within Smart Grid: An Overview," 2020 International Conference on Electrical, Communication, and Computer Engineering (ICECCE), Jun. 2020.

[8] A. J. Jahromi, M. R. Masoudi, M. Mohammadi, and S. Afrasiabi, "Improving electric vehicle charging forecasting: A hybrid deep learning approach for probabilistic predictions," IET Generation Transmission & Distribution, Oct. 2024.

[9] M. Rastegar, M. Fotuhi-Firuzabad, and F. Aminifar, "Load commitment in a smart home," Applied Energy, vol. 96, pp. 45–54, Feb. 2012.

[10] A. Viana and J. P. Pedroso, "A new MILP-based approach for unit commitment in power production planning," *International Journal of Electrical Power & Energy Systems*, vol. 44, no. 1, pp. 997–1005, Oct. 2012.

[11] G. W. Chang, Y. D. Tsai, C. Y. Lai, and J. S. Chung, "A practical mixed integer linear programming based approach for unit commitment," *IEEE Power Engineering Society General Meeting, 2004.*

[12] N. I. T. Halidou, N. H. or R. Howlader, N. M. E. Lotfy, N. A. Yona, and N. T. Senjyu, "Unit commitment in the presence of renewable energy sources and energy storage system: case study," *Journal of Energy and Power Engineering*, vol. 12, no. 6, Jun. 2018.

[13] A. Ademovic, S. Bisanovic, and M. Hajro, "A Genetic Algorithm solution to the Unit Commitment problem based on real-coded chromosomes and Fuzzy Optimization," *Melecon 2010 - 2010 15th IEEE Mediterranean Electrotechnical Conference*, Jan. 2010.

[14] J. Zhang, Q. Tang, Y. Chen, and S. Lin, "A hybrid particle swarm optimization with small population size to solve the optimal short-term hydro-thermal unit commitment problem," *Energy*, vol. 109, pp. 765–780, May 2016.

[15] A. Terki and H. Boubertakh, "A new hybrid Binary-Real coded Cuckoo search and Tabu search algorithm for solving the Unit-Commitment problem," *International Journal of Energy Optimization and Engineering*, vol. 10, no. 2, pp. 104–119, Apr. 2021.

[16] S. Arif, R. D. Mohammedi, A. Hellal, and A. Choucha, "A Memory Simulated Annealing Method to the Unit Commitment Problem with Ramp Constraints," *Arabian Journal for Science and Engineering*, vol. 37, no. 4, pp. 1021–1031, Apr. 2012.

[17] H. Xiong, Y. Shi, Z. Chen, C. Guo, and Y. Ding, "Multi-Stage robust dynamic unit commitment based on Pre-Extended -Fast robust dual dynamic programming," *IEEE Transactions on Power Systems*, vol. 38, no. 3, pp. 2411–2422, Jun. 2022.

[18] M. Carrion and J. M. Arroyo, "A computationally efficient Mixed-Integer linear formulation for the thermal unit commitment problem," *IEEE Transactions on Power Systems*, vol. 21, no. 3, pp. 1371–1378, Aug. 2006.

[19] Z.-K. Feng, W.-J. Niu, W.-C. Wang, J.-Z. Zhou, and C.-T. Cheng, "A mixed integer linear programming model for unit commitment of thermal plants with peak shaving operation aspect in regional power grid lack of flexible hydropower energy," *Energy*, vol. 175, pp. 618–629, Mar. 2019.

[20] D. Salman and M. Kusaf, *Day ahead unit commitment for IEEE-30 bus system application taking into consideration the uncertainty of wind power performance*. doi: 10.37247/pas.2.2022.30.